Polyhedron xxx (2013) xxx–xxx

Contents lists available at SciVerse ScienceDirect

Polyhedron

journal homepage: www.elsevier.com/locate/poly

Design of a bio-inspired copper (II) Schiff base complex grafted in mesoporous silica for catalytic oxidation

Wen-Juan Zhou [a,b,1], Belén Albela [a,*], Ming-Yuan He [b], Laurent Bonneviot [a,*]

[a] Laboratoire de Chimie, Ecole Normale Supérieure de Lyon, University of Lyon, 46, Allée d'Italie, 69364 Lyon Cedex 07, France
[b] Shanghai Key Lab of Green Chemistry and Chemical Processes, Department of Chemistry, East China Normal University, Shanghai, China

ARTICLE INFO

Article history:
Available online xxxx

Dedicated to Georges Christou for his 60th birthday.

Keywords:
MCM-41
Mesoporous silica
Copper complexes
Schiff base
Phenol hydroxylation

ABSTRACT

Controlled grafting of a copper (II) complex with a Schiff base ligand ($\mathbf{L_A}$ = *N*-(salicylaldimine)-(*N*′-propyltrimethoxysilane)-diethylenetriamine) on a mesoporous MCM-41 type of silica (LUS) was accomplished using a pattering technique to allow a homogeneous distribution of isolated copper sites on the solid using trimethylsilyl groups as dispersing function. XRD patterns suggest that the final material **LUS-Cu$\mathbf{L_A}$** exhibits a well-ordered 2D hexagonal structure. Elemental analysis, solid UV–Vis and EPR spectroscopies indicate that the copper (II) coordination sphere is most likely of a 3N1O type with an additional acetate ion as a ligand. Almost all the Cu(II) species grafted on the solid were EPR active (2.6 wt% active species for 2.8 wt% total copper measured from ICP-MS analysis) confirming the presence of monomeric copper species. Preliminary catalytic tests for phenol hydroxylation show that the supported system presents similar activity as the molecular analogue.

1. Introduction

The design of a heterogeneous catalyst with equivalent active sites and molecular control of the active species is a matter of concern. Indeed, better knowledge of the nature of the active sites can allow fine-tuning of the material to improve its reactivity properties and potential applications. Analogy with metalloproteins motivates research for the control of both structure of the metal sites and hydrophobicity at their vicinity. An obvious approach is to take advantage of recent progress in the grafting of homogeneous metal catalysts on inorganic supports to develop a bottom-up approach [1–7]. In particular, the use of a mesoporous silica matrix such as MCM-41 [8], MCM-48 [8] and SBA-15 [9], has allowed the synthesis of new heterogeneous catalysts [10–13]. Indeed, these solids are robust supports with a high specific surface area (600–1000 $m^2\ g^{-1}$) and small pore size distribution (pore diameter ~3–10 nm). In addition, they present the advantage of an easy functionalization with organic groups by grafting alkoxysilane derivatives on the silanol or silanolate functions (depending on the pH) at the pore-wall interface.

The most common approach consists in the grafting of either a ligand to be further complexed to the metal ion or a metal complex possessing one or two alkoxysilane arms [2–4,11,1]. In order to be successful using such approach, several conditions should be fulfilled: (i) a homogeneous distribution of the grafted species, (ii) a controlled environment of the metal ion, and (iii) a homogeneous confinement for the metal active sites. If these conditions are gathered, straightforward relations between structure and reactivity of the active sites can be stated and therefore an easy improvement of the material should be possible.

Homogeneous distribution of active sites implies isolation of the grafted species in the heterogeneous catalyst. Among the described strategies to isolate functions on a grafted porous silica, the so-called Molecular Stencil Pattering (MPS) approach offers the advantage of affording an homogeneous dispersion of one function at high loading [14–17]. The MPS has been developed for cationic templated mesoporous silica of MCM-41 type [18,19]. It is based on the use of the cationic template as stencil masking the surface according to a regular pattern generated by electrostatic self-repulsion. Then a sequential introduction of two different functions is performed: the first function is usually a trimethylsilyl (TMS) group, which acts as hydrophobic isolating function that is incorporated in the presence of some of the template molecules. Then, after removal of the remaining template molecules, the second function is introduced in the appropriate ratio to be totally surrounded by the first function, and therefore isolated. This approach has been already described for the synthesis of a heterogeneous ruthenium catalyst for sulfur oxidation [16].

Herein, we describe the grafting of a copper (II) Schiff base complex with the *N*-(salicylaldimine)-(*N*′-propyltrimethoxysilane)-diethylenetriamine ($\mathbf{L_A}$) ligand, using the MSP technique (Scheme 1).

* Corresponding authors. Tel.: +33 472 88 56/fax: +33 472 72 88 60.
E-mail address: belen.albela@ens-lyon.fr (B. Albela).
[1] Present address: Eco-Efficient Products and Processes (E2P2) Laboratory, 3966 Jin Du Rd., Xin Zhuang Industrial Zone, Shanghai 201108, China. Tel.: +86 21 24089535; fax: +86 21 54424351.

0277-5387/$ - see front matter © 2013 Elsevier Ltd. All rights reserved.
http://dx.doi.org/10.1016/j.poly.2013.06.039

This ligand has been chosen since it can mimic the metal environment of some oxidation copper metalloproteins such as catechol oxidase (GO) or copper amine oxidase (CAO) [20]. The aim of our work was the design of a heterogeneous catalyst for phenol hydroxylation. The challenge for this process is to be able to tune selectivity between catechol and hydroquinone, which are the desired products, and to diminish the formation of by-products such as tars.

2. Materials and methods

2.1. Chemicals and solutions

Copper (II) acetate monohydrate (99%, Acros), N^1-(3-trimethoxysilylpropyl) diethylenetriamine (**L_C**, 95%, ABCR), N'-isopropyldiethylenetriamine (tech., 75%, Aldrich), hexadecyltrimethylammonium-*p*-toluene-sulfonate, (CTATos; >99% Merck), Ludox HS-40 (40% SiO_2; Aldrich), hexamethyldisilazane (HMDSA, 98% Acros), sodium hydroxide (Acros), salicylaldehyde (98%, Avocado), ethyl alcohol anhydrous (plus for HPLC, Carlo Erba), hydrochloric acid (1 N standard solution, Acros), hydrogen peroxide (50% wt% solution in water, Aldrich), phenol (⩾99%, Sigma–Aldrich), catechol (99%, Acros), hydroquinone (⩾99%, Fluka), 1,4-benzoquinone (>99.5%, Fluka), potassium phosphate monobasic (99%, Acros), di-sodium hydrogen phosphate (anhydrous, Merck), sulfuric acid (95–97%, Fluka), Iotect (99%, Prolabo), potassium iodide (99%, Aldrich), potassium dichromate (99%, Avocado).

2.1.1. Sodium silicate solution

It was prepared as follows: Ludox (187 mL) was added to a solution of sodium hydroxide (32 g) in deionized water (800 mL) and stirred at 40 °C until clear.

2.1.2. Phosphate buffer solutions

(1) pH = 7: 0.68 g of KH_2PO_4 and 40 mL of 0.1 mol/L NaOH were introduced in a 100 mL volumetric flask. Distilled water was added until a total volume of 100 mL. [KH_2PO_4] = 50 mmol/L; (2) pH = 6: 2.085 g of KH_2PO_4 and 0.353 g of Na_2HPO_4 were introduced in a 250 mL volumetric flask. Distilled water was added until a total volume of 250 mL. [KH_2PO_4] = 60 mmol/L; (3) pH = 5: 0.2 mol/L of NaOH was added into 100 mL of KH_2PO_4 (0.2 mol/L); distilled water was added to adjust the pH until 5 controlled by pH-meter.

2.2. Synthesis of ligands HL_A and HL_B

A closed two-necked round flask with a condenser was firstly vacuumed at room temperature and then filled with argon. The same procedure was repeated for three times. Salicylaldehyde (1.09 mL, 10 mmol or 0.11 mL, 1 mmol) and absolute ethanol (50 mL) were injected in the flask. Then **L_C** (2.71 mL, 10 mmol) or N'-isopropyldiethylenetriamine (0.22 mL, 1 mmol) was dropwise added into the flask. The mixture was stirred under reflux for 6 h under argon atmosphere. The obtained yellow products were vacuumed and washed with a mixture of petroleum ether and ethyl acetate (7:2) and then vacuumed. The obtained yellow products were analyzed using ^{1}H NMR spectroscopy (Table S1).

2.3. Synthesis of complexes CuL_A and CuL_B

An ethanolic solution (10 mL) of HL_A (0.308 g, 0.73 mmol) or HL_B (0.199 g, 0.81 mmol) was introduced into a round flask. Then, copper acetate monohydrate (0.15 g, 0.74 mmol) in absolute ethanol (15 mL) was dropwise added. The resulting mixture was stirred under reflux for 2 h under argon atmosphere. Dark blue solutions containing **CuL_A** or **CuL_B** complexes were formed.

2.4. Synthesis of hybrids materials LUS-CuL_A and LUS-CuL_C

They were synthesized starting from a 2D hexagonal LUS silica prepared at 130 °C [18,19]. The Molecular Stencil Patterning (MSP) technique [14,16] was used to homogeneously distribute the grafted complexes, using trimethylsilyl functions (TMS) as isolating groups for the complexes (Fig. 1).

2.4.1. Synthesis of LUS

A sodium silicate solution (320 mL) was stirred at 60 °C for 1 h. A second solution of hexadecyltrimethylammonium p-tolunensulfonate (CTATos, 12.842 g) in deionized water (460 mL) was stirred during 1 h at 60 °C. The resulting solution was dropwise added to the second one during 20 min. The formed sol–gel was stirred at 60 °C for 24 h. After filtration and washing with deionized water (200–300 mL), the as-made solid was dried at 100 °C overnight, obtaining 19.8 g of **LUS**. Elemental analysis: C, 33.89; H, 6.72; N, 1.99%, weight loss at 1000 °C (48.38%).

2.4.2. Partial surfactant extraction

LUS (10 g) was placed in a round flask, and then ethanol (400 mL, 96%) and hydrochloric acid 1 mol L^{-1} (6.8 mL, 0.5 eq) were added. The mixture was stirred at 40 °C for 1 h. After filtration and washing with ethanol (100 mL × 2) and acetone (50 mL × 2) the solid was dried at 80 °C for 20 h. Material **LUS-PE** (7.1 g) was obtained.

2.4.3. Partial silylation

LUS-PE (6.8 g) was introduced in a round bottom three-necked flask, and then dried at 130 °C for 1 h under argon flow and during 2 h under vacuum. Cyclohexane (170 mL) and HMDSA (30 mL, 30 eq) were added under argon. The mixture was refluxed for 18 h. The obtained solid was finally washed with cyclohexane (2 × 30 mL), ethanol (2 × 60 mL) and acetone (2 × 60 mL), and then dried at 80 °C for 18 h. This sequence of steps was repeated twice. Finally, partially silylated material **LUS-PES** (7.1 g) was obtained.

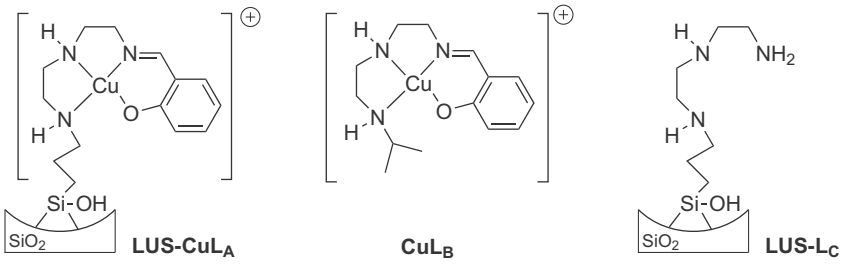

Scheme 1. Structure of the grafted species LUS-CuL_A and LUS-L_C and the molecular analogue CuL_B.

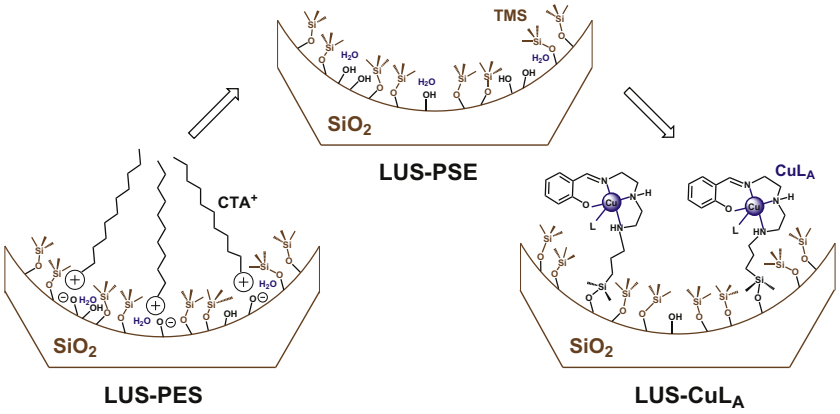

Fig. 1. Synthesis route to prepare **LUS-CuL_A** using the MSP approach. A perpendicular section of the pore of the mesostructured silica LUS is represented.

2.4.4. Extraction of the remaining surfactant

LUS-PES (2 g) was placed in a round flask, and then ethanol (86 mL, 96%) and hydrochloric acid (1.28 mL, 1 eq, 1 mol/L) were added. The mixture was stirred at 0 °C for 1 h. After filtration and washing with ethanol (50 mL) and acetone (50 mL) the obtained solid was dried at 80 °C for 20 h. The same procedure was repeated again. Finally, material **LUS-PSE** (1.4 g) was obtained. Elemental analysis: C, 7.72; H, 2.40; N, <0.1%, weight loss at 1000 °C (10.33%).

2.4.5. Grafting of the complex Cu-L_A

LUS-PSE (0.5 g) was dried at 130 °C under argon flow during 1 h, and then vacuumed at 130 °C during 2 h. A solution of metal complex (0.74 mmol of **Cu-L_A** complex) in 2 mL anhydrous ethanol was added into the flask together with 40 mL of toluene. The resulting mixture was stirred at 60 °C for 18 h under argon. The obtained solid was washed with toluene (50 mL) and ethanol (25 mL), and then dried at 60 °C overnight, obtaining material **LUS-CuL_A** (0.55 g). Elemental analysis: C, 13.82; N, 1.92; Cu, 2.8%, weight loss at 1000 °C (18.12%).

2.4.6. Grafting of ligand L_C

LUS-PSE (0.3 g) was dried at 130 °C under argon flow during 1 h, and then vacuumed at 130 °C during 2 h. Ligand **L_C** (0.07 mL) was added into the flask together with 50 mL of toluene. The resulting mixture was stirred at 60 °C for 18 h under argon. The obtained solid was washed with toluene (50 mL) and ethanol (25 mL), and then dried at 60 °C overnight, obtaining material **LUS-L_C** (0.33 g).

2.5. Catalytic tests

Phenol hydroxylation experiments were run in a 50 mL two-necked flask with a condenser. In a standard run, phenol (0.1 g, 1.1 mmol), catalyst [Cu:phenol = 1:100, **LUS-CuL_A**] and buffer solution (see above for composition, 7 mL) and H_2O_2 (50% aqueous) were orderly added. The reaction was carried out at 80 °C for 2 h. Phenol and the possible products, catechol (CAT), hydroquinone (HQ) and 1,4-benzoquinone (BQ), were analyzed by HPLC. H_2O_2 conversion was determined by the following methods: (i) the H_2O_2 conversion was determined by iodometry method, and (ii) the efficiency conversion of H_2O_2 was calculated as follows: H_2O_2 eff. conv. = 100 × H_2O_2 (mol) consumed in formation of diphenols and benzoquinone/H_2O_2 (mol) converted.

2.6. Analytical techniques

Low angle X-ray powder diffraction (XRD) experiments were carried out using a Bruker (Siemens) D5005 diffractometer using Cu K monochromatic radiation. Infrared (IR) spectra were recorded from KBr pellets using a Mattson 3000 IRTF spectrometer. Liquid UV–Vis spectra were recorded using a Vector 550 Bruker spectrometer; solid diffuse reflectance UV–Vis spectra were recorded from aluminum cells with Suprasil 300 quartz windows, using a PerkinElmer Lambda 950 spectrophotometer and PE Winlab software. Nitrogen sorption isotherms at 77 K were determined with a volume device Micromeritics ASAP 2010 M on solids that were dried at 80 °C under vacuum overnight. TGA measurements were collected from Al_2O_3 crucibles on a DTA-TG Netzsch STA 409 PC/PG instrument, under air (30 mL/min), with a 25–1000 °C (10 °C / min) temperature increase. pH-meter (Meterlab pHM210) was calibrated in aqueous solution. EPR spectra were recorded using a Brucker Elexsys e500 X-band (9.4 GHz) spectrometer with a standard cavity. Quantification of Cu(II) species was performed using crystals of $CuSO_4{\cdot}5H_2O$ as calibration reference. ^{1}H NMR spectra were recorded on a Brucker Advance 300 NMR spectrometer. HPLC analyses were performed on a LC/MS Agilent 1100SLT. The working conditions were the following: column, ZORBAX-SB-C_{18} of dimension 4.6 × 250 mm; protect, 5 microns; loop size, 8 μL; temperature of the column, room temperature; UV detector, λ = 245 nm and 280 nm; mobile phase, water (10 mmol L^{-1} formic acid, 60%) and acetonitrile (40%); flow rate, 0.2 mL min^{-1}.

3. Results and discussion

3.1. Synthesis of the hybrid materials containing the copper complex

The ligand H**L_A** was synthesized starting from N^1-(3-trimethoxysilylpropyl) diethylenetriamine (**L_C**), and it was complexed with copper (II) acetate prior to the grafting. The hybrid material possessing the desired **CuL_A** sites (Scheme 1) was prepared using LUS silica as inorganic support, which is a 2D hexagonal mesostructured porous silica (MCM-41 type) that is synthesized in basic conditions using cetyltrimethylammonium tosylate (CTATos) as template to generate the mesoporosity. Then the molecular stencil patterning (MSP) technique was used to introduce, first trimethylsilyl (TMS) groups as isolating functions, and second, the copper (II) complex **CuL_A** precursor [6,16]. In the first step, the cationic template (CTA^+) that covers the surface of **LUS** was partially removed by adding an appropriate amount of HCl, obtaining **LUS-PE** material (Fig. 1). In the second step, TMS groups were grafted in the empty space without removal of the remaining

template molecules that act as stencil, leading to **LUS-PES**. In the third step, the remaining template molecules were extracted by adding a suitable amount of HCl in gentle conditions (1 h at 0 °C) to afford **LUS-PSE**. Finally, the **CuL$_A$** complex was grafted on the partially silylated mesoporous material (**LUS-CuL$_A$**). A molecular analogue without the silane arm, *i.e.* **CuL$_B$**, and the corresponding hybrid material with **L$_C$** ligand (precursor of H**L$_A$**), *i.e.* **LUS-L$_C$**, were also synthesized to better characterize the desired material **LUS-CuL$_A$** (Scheme 1).

3.2. Characterization of the copper materials

An appropriate TMS/**CuL$_A$** ratio was required to lead to isolated metal complexes totally surrounded by TMS functions. In the final material **LUS-CuL$_A$** this ratio was of 3.5 (Table S2), as deduced from chemical analysis and quantitative IR spectroscopy, with ~80% of the surface covered with organic functions (TMS + L$_A$). The L$_A$/Cu molar ratio of 1.0 in the initial synthesis gel was conserved in the final material. Almost all the Cu(II) species grafted on the solid were EPR active (2.6 wt% active species for 2.8 wt% total copper measured from ICP-MS analysis, Table S2, *vide infra*). IR spectroscopy confirmed the presence of L$_A$ ligand and suggested the retention of acetate ions in the solid (Fig. S1). Indeed, a phenolate stretching vibration band was observed at 1542 cm^{-1} characteristic of metal-salen complexes [21,22] and a band at 1451 cm^{-1} likely assigned to the deformation vibration of the aromatic ring [23]. An additional band was observed at 1640 cm^{-1} compared to the reference material **LUS-L$_C$**, which is likely attributed to the ν(C=N) of the imine function after incorporation of **CuL$_A$**, discarding a possible hydrolysis of the imine group present in **L$_A$** during the synthesis of the hybrid material [24,25]. The presence of acetate ions in the solid was stated from the observation of the two characteristic symmetrical $\nu_s(CO_2^-)$ and asymmetrical $\nu_{as}(CO_2^-)$ stretching vibrations of the carboxylate group at 1400 and 1605 cm^{-1}, respectively [26]. The separation between these two bands ($\Delta\nu$ ~200 cm^{-1}) is much larger than for the free acetate ion ($\Delta\nu$ = 144 cm^{-1}, $\nu_a(CO_2^-)$: 1560 cm^{-1}, $\nu_s(CO_2^-)$: 1416 cm^{-1}), which is in accordance with a monodentate acetate ion coordinated to the metal ion [26,27]. These results combined with those from elemental analyses allowed us to conclude that only one acetate ion was retained in **LUS-CuL$_A$** material to neutralize the charge of the Cu(II) complex.

The integrity of the copper complex in **LUS-CuL$_A$** was confirmed by UV–Vis spectroscopy (Fig. 2). Indeed, **LUS-CuL$_A$** displays a broad absorption band below 330 nm, which can be attributed to ligand-based π–π^* transitions. A second band at *ca.* 370 nm was observed, which was also present for the molecular species **CuL$_A$** in ethanol, but that was absent fort the free ligand H**L$_A$**. This band can be assigned to a n–π^* transition of the imino group coordinated to the Cu ion [24]. Finally, the broad absorption band at *ca.* 588 nm, which was also observed in complex **CuL$_A$**, corresponds to the d–d transitions of the Cu(II) ion.

The EPR spectrum observed for **LUS-CuL$_A$** is typical of d^9 complexes with $d_{x^2-y^2}$ ground state and elongated square pyramidal or elongated octahedral environment for Cu(II) (Fig. 3). Indeed, values of $g_{||}$, $g_\perp$ and $A_{||}$ of **LUS-CuL$_A$** were equal to 2.18, 1.99 and 19.4 mT at room temperature, and slightly changed to 2.20, 1.98 and 19.5 mT at 130 K, which are similar to those observed for the **CuL$_B$** complex. In addition, EPR spectra become broaden at low temperature (130 K). The reason is most probably that at low temperature the grafted complex possesses low mobility and is blocked in various conformations due to the heterogeneity of the silanol and TMS position in its vicinity. Different parameters of $g_{||}$ and $A_{||}$ of Cu(II) complexes in EPR spectra can be attributed to a varying number of nitrogen and oxygen coordinating sites and to a change in the symmetry around the metal center. Moreno-Carretero et al. have reported that 6-amino-l,3-dimethyl-5-nitrosouracilato (N^5, N^6)-aqua-2,2′-bipyridine (*N*,*N*′)-copper (II) perchlorate hydrate and 2,2′-bipyridine(*N*,*N*′)-chloro-l,3-dimethylviolurato(N^5, O^6)-copper (II) hemihydrate complexes display axial EPR powder spectra with $g_\perp$ = 2.03 and $g_{||}$ = 2.25 and $g_\perp$ = 2.03 and $g_{||}$ = 2.20, respectively, proposing a $(4N)_{xy} + O_z$ and $(3N1O)_{xy} + O_z$ environment around the Cu(II) [28]. Abry et al. have observed that *N*,*N*′-bis(2-pyridinylmethyl)-ethane-1,2-diamine copper (II)trifluoromethanesulfonate complex with tetradentate ligand grafted in mesoporous silica exhibits low g values with $g_{||}$ = 2.219 and $g_\perp$ = 1.994 [29]. Combining EPR spectra with EXAFS analysis, they proposed a 2N2O environment for the grafted copper complexes. For **LUS-CuL$_A$**, it seems that a $(3N1O)_{xy} + O_z$ environment around copper is more reasonable than $(2N2O)_{xy}$ and the coordination geometry is rather pentacoordinated.

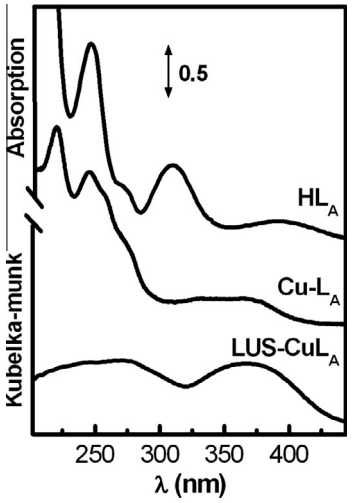

Fig. 2. Liquid UV–Vis spectra of **HL$_A$** and **Cu-L$_A$** in absolute ethanol and solid diffuse reflectance UV–Vis spectra of **LUS-CuL$_A$**.

The hybrid material **LUS-CuL$_A$** possesses a highly ordered 2D hexagonal mesostructure, as shown in the XRD pattern with the presence of the characteristic (100), (110) and (200) diffractions (a_0 = 4.7 nm) (Fig. 4, left). Nitrogen sorption isotherms for **LUS-CuL$_A$** and the intermediate materials during the synthesis of the hybrid catalyst were of type IV according to the IUPAC

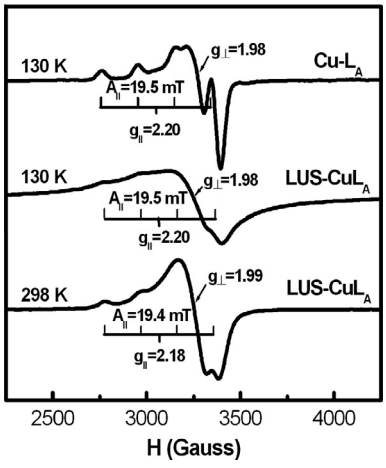

Fig. 3. Solid state EPR spectra of **Cu-L$_A$** and **LUS-CuL$_A$**. The spectra were recorded at 130 K for the former sample, and at 130 K and room temperature respectively for the latter. Frequency: 9.35 GHz; power: 10, 32 and 10 mW, respectively; modulation amplitude: 6G, 15G and 1G respectively, and modulation frequency: 100 kHz.

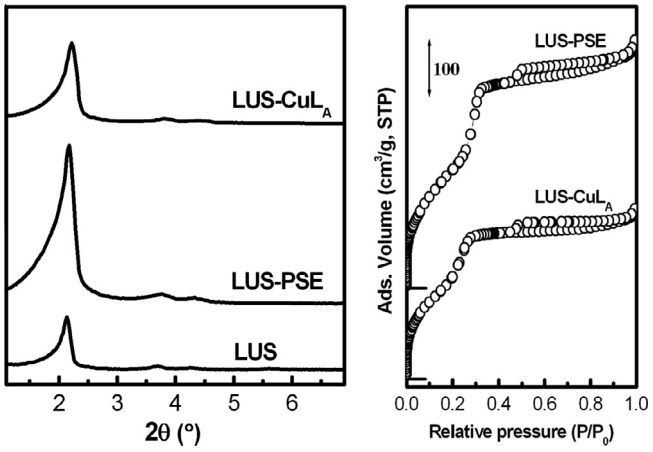

Fig. 4. XRD patterns of **LUS**, **LUS-PSE** and **LUS-CuL$_A$** (left), and N_2 sorption isotherms of **LUS-PSE** and **LUS-CuL$_A$** at 77 K (right).

classification (Fig. 4, right) [30]. The steep step of the capillary condensation at about 0.38 P/P_0 evidences a narrow pore size distribution (Table S3) [8,31]. The specific surface (S_{BET}) and total pore volume of **LUS-CuL$_A$** are 660 $m^2\ g^{-1}$ and 0.45 $cm^3\ g^{-1}$, respectively. These values are lower than those corresponding to the parent support **LUS-PSE** (820 $m^2\ g^{-1}$ and 0.66 $cm^3\ g^{-1}$), indicating the incorporation of the metal complexes inside the pores of the silica. Consistently, the pore diameter ϕ_{BdB} (Broekhoff and de Boer model) was reduced from 3.2 nm for **LUS-PSE** to 2.8 nm for **LUS-CuL$_A$**, upon incorporation of the complex. This shows that the metal complexes are effectively inside the pores while there is still enough space for the catalytic reaction to take place.

3.3. Catalytic activity

The catalytic activity of **LUS-CuL$_A$** was evaluated for phenol hydroxylation with H_2O_2 (50 wt%) in diluted aqueous conditions with an average initial phenol concentration of 1.4 wt% in a phosphate buffer. A reaction time of 2 h at 80 °C with a H_2O_2/phenol molar ratio of one, using 1 mol% of **LUS-CuL$_A$** catalyst was investigated. The formed products were analyzed using HPLC. In addition to the catechol (CAT), hydroquinone (HQ) and 1,4-benzoquinone (BQ), dark brown by-products were also observed [32,33]. These products may be the result of over-oxidation, coupling of radical intermediates and cleavage of oxidation products, for example maleic acid, acrylic acid, acetic acid, oxalic acid, polyphenols and other oligomers, that are usually called as tar [34].

Considering that no activity on phenol hydroxylation was reported at pH >9 over hydrotalcite-like compounds ($CuAlCO_3$-HTLc) and ternary hydrotalcites (CuNiAl or CuCoAl) [11], pH was limited to the range 5–7 for the catalyst here studied. The phenol conversion increased from 21% to 43% and to 51% when the pH was decreased from 7.0 to 6.0 and further to 5.0 (Table S4). However, the highest diphenols selectivity was observed at pH = 6.0, *i.e.*, 73%. Therefore, a good compromise between phenol conversion and diphenol selectivity was to run the reaction at pH 6.

Without catalyst or with TMS-modified mesoporous silica (**LUS-PSE**) there was a low phenol conversion (~12%) and no diphenol formation (entries 1–2, Table 1). The molecular analogue **CuL$_B$** and the supported catalyst exhibited much higher phenol conversion (~50%) and a high selectivity in diphenol (~70–80%) with a CAT/HQ molar ratio of ~1.6 in both cases (entries 3–4, Table 1).

Next the variation of the substrate/oxidant molar ratio was investigated. Increasing the amount of oxidant, improves phenol conversion for a lower H_2O_2 efficiency and lower diphenols selectivity, in agreement with previous works [10,12]. The turnover numbers (TON) were comprised between 11 and 38, increasing for higher amounts of oxidant present in the reaction mixture (Table 2). Conversely, the highest diphenol selectivity of ca. 76% was observed when less oxidant was used up to a phenol/H_2O_2 molar ratio of 1.2 (entries 1–4, Table 2). The CAT/HQ ratio was not very sensitive to this parameter, which differs from results reported on TS-1 zeolite, where this ratio strongly decreases for higher amount of H_2O_2 [12]. Adding H_2O_2 stepwise or at once, was investigated since it was reported to affect both activity and selectivity [10,13]. Sequential addition of H_2O_2 for 1 h at the reaction temperature mainly impacted on diphenol selectivity which decreased from 73% (one addition) down to 55% (sequential), while phenol conversion and CAT/HQ ratio were practically not affected (entries 2–2*, Table 2). These results suggest that sequential addition favors the formation of by-products at the expense of CAT and HQ.

Finally, a recycling test was performed on the catalyst filtered and washed with ethanol and acetone, and dried overnight at 60 °C before the next run. After the second run, the catalyst retains all the catalytic properties (entries 2–2′, Table 2). However, at the third run, the activity decreases by 20% (entry 2″). Indeed, after the

Table 1
Comparison of the catalytic activity of **LUS-CuL$_A$** with other systems.

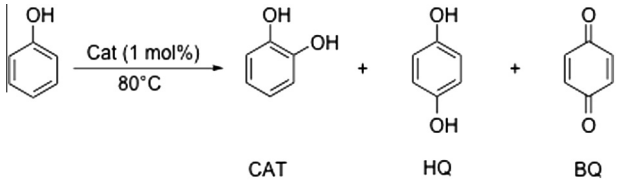

Entry	Catalyst	Phenol conv. (%)	Diphenols selectivity (%)	Product selectivity (%)			CAT/HQ
				CAT	HQ	BQ	
1	No catalyst	11	0	0	0	0	0
2	LUS-PSE	12	0	0	0	0	0
3	Cu-L$_B$	52	70	61	39	0.2	1.6
4	LUS-CuL$_A$	48	76	63	37	0	1.7

All the reactions were performed at 80 °C and pH = 6 in a phosphate buffer (60 mM) solution; reaction time 2 h; phenol: H_2O_2 = 1: 1.2 (molar ratio); H_2O_2 was added at once. Products were analyzed using HPLC. [b] Diphenols selectivity = yield of CAT, HQ and BQ/phenol conversion (mol%). Relative precision ~10%. CAT: catechol; HQ: hydroquinone; BQ: 1, 4-benzoquinone.

Table 2
Effect of the phenol:H_2O_2 molar ratio on the catalytic activity of **LUS-CuL$_A$** and recycling test.

Entry	Phenol/H_2O_2	Phenol Conversion (%)	H_2O_2 eff. Conv. (%)	Diphenols selectivity (%)	CAT/HQ	TON
1	1:1/3	15	34	73	2.0	11
2	1:1	43	31	73	1.6	13
2*	1:1	41	n.d.	55	1.7	23
2′[a]	1:1	43	30	71	1.7	30
2″[a]	1:1	33	20	62	1.9	20
3	1:1.2	48	31	76	1.8	36
4	1:2.2	73	25	52	1.6	38

The reactions were performed at 80 °C, using 1 mol% Cu catalyst (LUS-CuL$_A$), phenol: H_2O_2 = 1:1, reaction time 2 h, pH = 6 in phosphate buffer solution (60 mM). H_2O_2 conversion = mol H_2O_2 consumed to form diphenols/mol H_2O_2 converted (mol%). Diphenols selectivity = yield of CAT and HQ/phenol conversion (mol%). 2*: Sequential addition of H_2O_2 for 1 h; in all the other cases it was added at once.

[a] Recycling test of 2 (2′: second run, 2″: third run). N.d. = non determined. Relative precision ~10%. CAT: catechol; HQ: hydroquinone. TON: turnover number.

first run, most of the TMS functions (~99%) were lost though the copper ions were retained according to elemental analysis and they were complexed to $\mathbf{L_A}$ according to EPR spectroscopy analysis (Fig. S2). The mesostructure of the solid was also retained since no modification of the XRD pattern was observed (Fig. S3). The partial loss of hydrophobic functions (TMS) likely favors metal leaching, which can explain the decrease of the catalytic activity after the second run. In addition, a broad absorption band from 200 to 800 nm was observed in the UV–Vis spectrum of the recycled catalysts, due to the presence of tar in the solid, consistent with the dark brown coloration of the solid after the reaction. This tar also contributes to the decrease of the catalytic activity of the solid by plugging the pore entrance and therefore diminishing the access to the active sites.

4. Conclusions

It is shown here that the design of a heterogeneous catalyst using a bio-inspired metal complex may encounter a reasonable success by combining molecular control on the metal environment with hydrophobization of its vicinity. This is exemplified here using a tetradentate copper Schiff base complex grafted on MCM-41 type of silica, the surface of which has been partially hydrophobized using the molecular stencil patterning technique. Copper sites are isolated in the solid and no pair forming has been observed. The hybrid material possesses a structured porosity and a high porous volume, which allows its use in catalysis. Indeed, it exhibits very similar catalytic activity as the molecular analogue in phenol hydroxylation using H_2O_2 as oxidant. Recycling tests show that loss of hydrophobic trimethylsilyl functions after the first run favors metal leaching, which together with the presence of tar in the solid diminishes its catalytic activity after the second run. Studies are in progress to develop new robust hydrophobic functions to improve such heterogeneous catalysts.

Acknowledgments

JoRISS cooperative program between Ecole Normale Supérieure (ENS) of Lyon (France) and East China Normal University (ECNU) in Shanghai (China). W.Z. thanks both French and Chinese Governments for Doctoral Scholarships.

Appendix A. Supplementary data

Supplementary data associated with this article can be found, in the online version, at http://dx.doi.org/10.1016/j.poly.2013.06.039.

References

[1] D. Brunel, Microporous Mesoporous Mater. 27 (1999) 329.
[2] X.G. Zhou, X.Q. Yu, J.S. Huang, S.G. Li, L.S. Li, C.M. Che, Chem. Commun. (1999) 1789.
[3] R.I. Kureshy, I. Ahmad, N.H. Khan, S.H.R. Abdi, K. Pathak, R.V. Jasra, J. Catal. 238 (2006) 134.
[4] T.J. Terry, T.D.P. Stack, J. Am. Chem. Soc. 130 (2008) 4945.
[5] C. Li, H.D. Zhang, D.M. Jiang, Q.H. Yang, Chem. Commun. (2007) 547.
[6] S. Abry, F. Lux, B. Albela, A. Artigas-Miquel, S. Nicolas, B. Jarry, P. Perriat, G. Lemercier, L. Bonneviot, Chem. Mater. 21 (2009) 2349.
[7] P. Barbaro, F. Liguori, Heterogenized Homogeneous Catalysts for Fine Chemicals Production: Materials and Processes, Springer, Netherlands, 2010.
[8] J.S. Beck, J.C. Vartuli, W.J. Roth, M.E. Leonowicz, C.T. Kresge, K.D. Schmitt, C.T.W. Chu, D.H. Olson, E.W. Sheppard, S.B. McCullen, J.B. Higgins, J.L. Schlenker, J. Am. Chem. Soc. 114 (1992) 10834.
[9] D.Y. Zhao, J.L. Feng, Q.S. Huo, N. Melosh, G.H. Fredrickson, B.F. Chmelka, G.D. Stucky, Science 279 (1998) 548.
[10] K. Moller, T. Bein, Chem. Mater. 10 (1998) 2950.
[11] D. Brunel, N. Bellocq, P. Sutra, A. Cauvel, M. Lasperas, P. Moreau, F. Di Renzo, A. Galarneau, F. Fajula, Coord. Chem. Rev. 178 (1998) 1085.
[12] K. Ariga, A. Vinu, J.P. Hill, T. Mori, Coord. Chem. Rev. 251 (2007) 2562.
[13] A. Taguchi, F. Schuth, Microporous Mesoporous Mater. 77 (2005) 1.
[14] S. Abry, A. Thibon, B. Albela, P. Delichere, F. Banse, L. Bonneviot, New J. Chem. 33 (2009) 484.
[15] W.J. Zhou, B. Albela, M. Ou, P. Perriat, M.Y. He, L. Bonneviot, J. Mater. Chem. 19 (2009) 7308.
[16] S. Calmettes, B. Albela, O. Hamelin, S. Menage, F. Miomandre, L. Bonneviot, New J. Chem. 32 (2008) 727.
[17] K. Zhang, B. Albela, M.Y. He, Y.M. Wang, L. Bonneviot, Phys. Chem. Chem. Phys. 11 (2009) 2912.
[18] L. Bonneviot, M. Morin, A. Badiei, Patent WO 01/55031 A 1, (2001).
[19] L. Bonneviot, A. Badiei, N. Crowther, Patent WO 02216267, (2002).
[20] E.I. Solomon, U.M. Sundaram, T.E. Machonkin, Chem. Rev. 96 (1996) 2563.
[21] C. Baleizao, B. Gigante, H. Garcia, A. Corma, Tetrahedron Lett. 44 (2003) 6813.
[22] C. Baleizao, B. Gigante, D. Das, M. Alvaro, H. Garcia, A. Corma, J. Catal. 223 (2004) 106.
[23] S. Walas, A. Tobiasz, M. Gawin, B. Trzewik, M. Strojny, H. Mrowiec, Talanta 76 (2008) 96.
[24] W.J. Zhou, B. Albela, P. Perriat, M.Y. He, L. Bonneviot, Langmuir 26 (2010) 13493.
[25] H. Miyasaka, S. Okamura, T. Nakashima, N. Matsumoto, Inorg. Chem. 36 (1997) 4329.
[26] J.E. Tackett, Appl. Spectrosc. 43 (1989) 483.
[27] K. Nakamoto, Infrared and Raman Spectra of Inorganic and Coordination Compounds. Part B: Applications in Coordination, Organometallic, and Bioinorganic chemistry, fifth ed., Wiley, 1992.
[28] F. Belanger-Gariepy, R. Faure, F. Hueso-Urena, M.N. Moreno-Carretero, J.A. Rodriguez-Navarro, J.M. Salas-Peregrin, Polyhedron 17 (1998) 1747.
[29] S. Abry, A. Thibon, B. Albela, P. Delichère, F. Banse, L. Bonneviot, New J. Chem. 33 (2009) 484.
[30] K.S.W. Sing, D.H. Everett, R.A.W. Haul, L. Moscou, R.A. Pierotti, J. Rouquerol, T. Siemieniewska, Pure Appl. Chem. 57 (1985) 603.
[31] C.T. Kresge, J.C. Vartuli, W.J. Roth, M.E. Leonowicz, The discovery of ExxonMobil's M41S family of mesoporous molecular sieves, in: O.Terasaki (Ed.), Mesoporous Crystals and Related Nano-Structured Materials, Elsevier, 2004, pp. 53–72.
[32] F.S. Xiao, J.M. Sun, X.J. Meng, R.B. Yu, H.M. Yuan, J.N. Xu, T.Y. Song, D.Z. Jiang, R.R. Xu, J. Catal. 199 (2001) 273.
[33] J.A. Martens, P. Buskens, P.A. Jacobs, A. Vanderpol, J.H.C. Vanhooff, C. Ferrini, H.W. Kouwenhoven, P.J. Kooyman, H. Vanbekkum, Appl. Catal. 99 (1993) 71.
[34] A. Santos, P. Yustos, A. Quintanilla, S. Rodriguez, F. Garcia-Ochoa, Appl. Catal. B 39 (2002) 97.